ENERGETICS OF A SUBSTORM ON 15 AUGUST, 2001: COMPARING EMPIRICAL METHODS AND A GLOBAL MHD SIMULATION

E. I. Tanskanen[1,2], M. Palmroth[2], T.I. Pulkkinen[2], H.E.J. Koskinen[3,2], P. Janhunen[2], N. Østgaard[4], J.A. Slavin[1], K. Liou[5]

[1]*NASA GSFC, Code 696, Greenbelt, Maryland, USA*
[2]*Finnish Meteorological Institute, Space Research Unit, Helsinki, Finland*
[3]*University of Helsinki, Department of Physics, Helsinki, Finland*
[4]*Space Science Laboratory, University of California, Berkeley, California, USA*
[5]*Johns Hopkins University, Applied Physics Laboratory, Laurel, Maryland, USA*

ABSTRACT

Energy transferred from the solar wind into the magnetosphere-ionosphere system is dissipated largely through the occurrence of substorms. In this paper a substorm that occurred on 15 August, 2001, between 0220 and 0620 UT is analyzed using several empirical estimates for energy input, for Joule heating and for electron precipitation. The total energy input is estimated in terms of Akasofu's epsilon parameter, with original scaling parameter $l_0 = 7\ R_E$ and revised scaling $l_0 = 10\ R_E$. Empirically estimated energy input is compared to the results of a GUMICS-4 global MHD simulation. Temporal variation of the input curves compare favorably during substorm growth and expansion phases, while there are differences during the substorm recovery phase. Global electron energy dissipation given by PIXIE on board the POLAR spacecraft matches nicely to the results of the GUMICS-4 simulation in temporal variations, but the absolute levels of dissipation are quite different.

INTRODUCTION

First empirical estimates of the magnetospheric energy input and sinks were developed in the late 1970's and early 1980's (Perreault and Akasofu, 1978; Akasofu, 1981; Ahn et al., 1983). Since that time the estimates for the ionospheric energy sinks have evolved significantly. Most Joule heating estimates are based on ground magnetic measurements while estimates for the electron precipitation are based for both radar and spacecraft measurements. The method developed by Ahn et al. (1983) for estimating the electron precipitation is based on Chatanika radar measurements, Spiro et al. (1982) used measurements from the low energy electron experiment on board Explorer C and D spacecraft, while one of the most recent methods, created by Østgaard et al. (2002), is based on POLAR satellite UV and X-ray imaging.

Besides improved estimates for Joule heating, electron precipitation and ring current, some new energy sinks have been discovered. In the early 1980's the ISEE mission provided novel observations of tailward moving plasmoids (Hones et al. 1984; Scholer et al. 1984). In addition to the energy carried inside the plasmoid, the post-plasmoid plasma-sheet has a significant contribution to substorm energetics (Richardson et al., 1987). In fact, the energy carried by the ejected plasmoid and the post-plasmoid tailward flows can be comparable to the energy dissipated in the ionosphere during substorms (Slavin et al. 1993; Ieda et al. 1998). Recently, Koskinen and Tanskanen (2002) suggested that ϵ should be slightly revised to account for the substorm-related tail energy sinks. For the purpose of this paper the original and the rescaled epsilon, ϵ_{scaled}, is used for estimating the input energy. Empirical input estimates are compared to the energy transferred through the magnetopause as evaluated from the GUMICS-4 simulation.

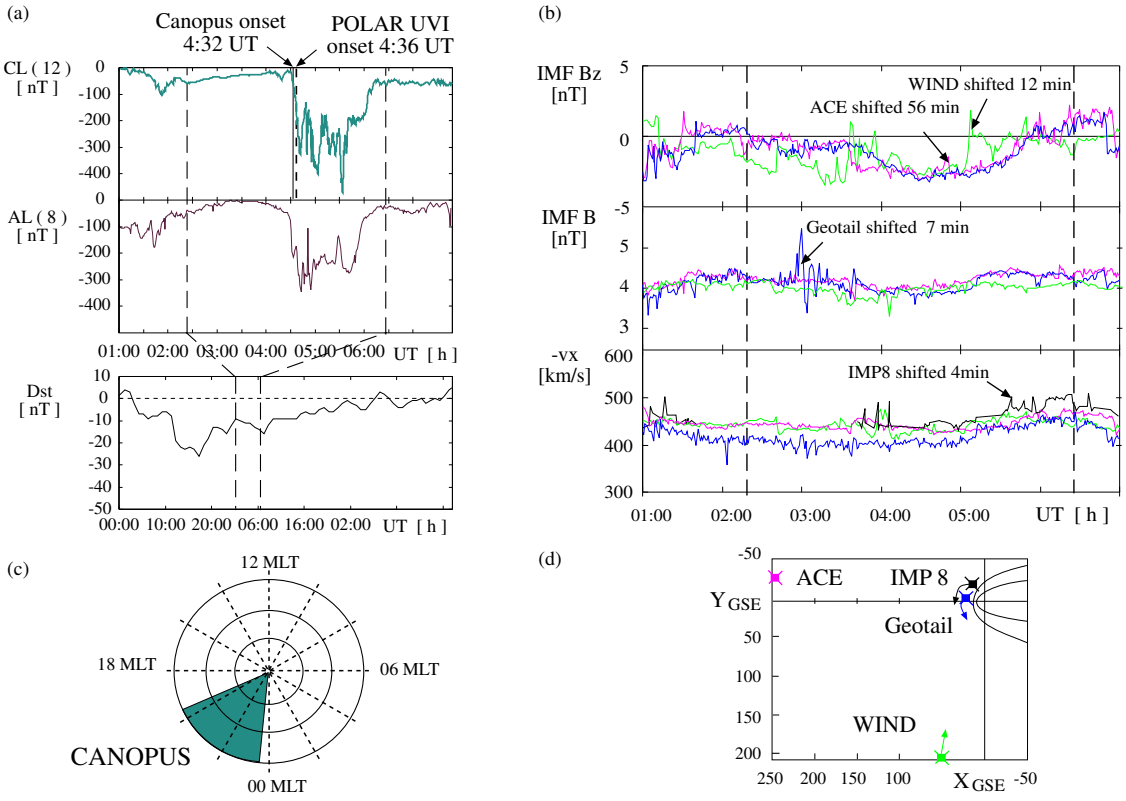

Fig. 1. (a) CANOPUS and AE-chain measurements. (b) Geotail, ACE, IMP 8 and WIND observations. (c) CANOPUS and AE locations. (d) ACE, Geotail, IMP 8 and WIND locations.

EVENT DESCRIPTION: A SUBSTORM ON 15 AUGUST 2001

Ground-based measurements

A medium-size substorm was observed on 15 August, 2001 between 0220 UT and 0620 UT. AE and CANOPUS chains observed a clear magnetic bay with sharp decrease of the westward electrojet indices (AL and CL in Figure 1a). The CANOPUS magnetometer array was located in the pre-midnight sector, where the main activity occurred. The main substorm onset was observed in the AL and CL indices almost simultaneously at 0430 UT and 0432 UT, respectively. The CL-index is an envelope curve formed from the measurements of a north-south component of twelve CANOPUS array observatories (TALO, CONT, DAWN, RANK, FSIM, ESKI, FSMI, FCHU, RABB, MCMU, GILL and ISSL). At each instant of time the lowest value of the north-south component, X, is selected. The intensity of the substom, max(|CL|) was about 450 nT. Around the onset the CL decreased about 300 nT in less than 10 minutes. Figure 1a also shows the Dst index, which reflects the ring current intensity. The substorm occurred during the recovery phase of a very weak storm, Dst index being around -10 nT during the entire substorm event.

Solar wind measurements

Magnetic field and solar wind velocity measurement were recorded by 4 upstream spacecraft: ACE, Geotail, IMP 8 and WIND. ACE located at the L1 point (GSE 242, -32, 25 R_E), Geotail and IMP 8 near the magnetopause (GSE 21, -6, 1 R_E and GSE 16, -25, -27 R_E, respectively) and WIND about 200 R_E in the dusk sector (53, 229, -20 R_E). In Figure 1b we present interplanetary magnetic field (IMF) B_z component, the total strength of the IMF, B, and x-component of the velocity, v_x. All data are time shifted to the magnetopause at 10 R_e by using the average v_x during the event to account for the solar wind convection to the Earth. All the parameters measured by the four spacecraft showed similarities, even the spacecraft were far apart from each other. However, the fine structure in the velocities and magnetic fields were slightly less correlated: Linear correlation coefficients between ACE and Geotail during the substorm period for B_z, B

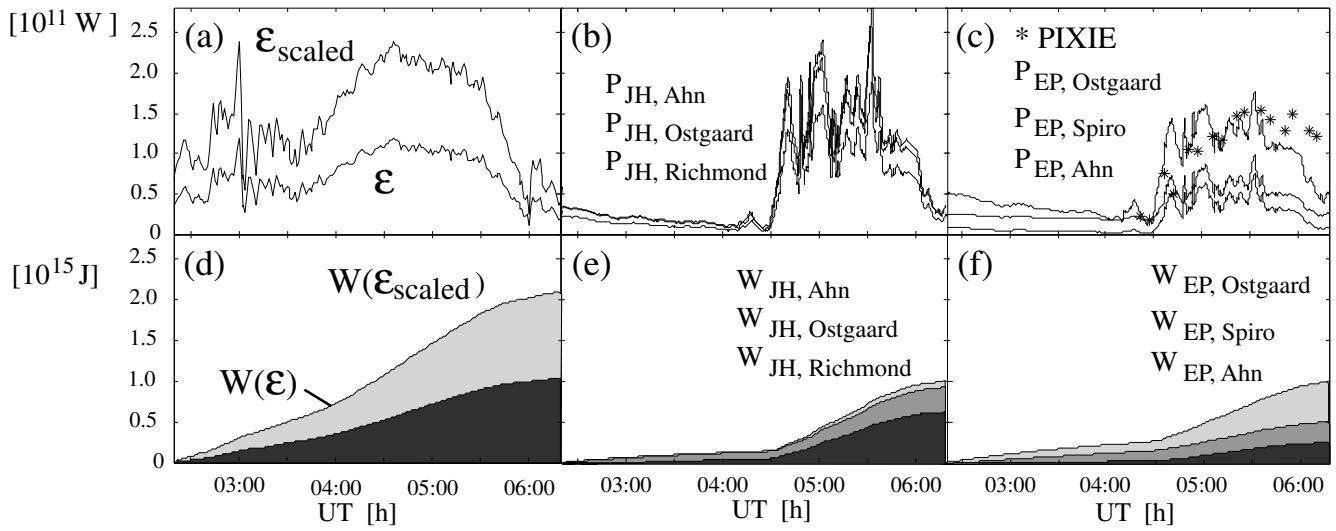

Fig. 2. Solar wind energy input (a), Joule heating (b), and electron precipitation (c) together with the integrated total energy for solar wind input (d), Joule heating (e), and electron precipitation (f). Two different formulas are used for solar wind input computation, since three formulas are presented for Joule heating and for electron precipitation. The methods are listed due to their magnitude. In addition, electron precipitation based on PIXIE measurements is presented with asterisks.

and v_x were 0.74, 0.85 and 0.84, respectively, while the correlation coefficients between Geotail and WIND were 0.36, 0.71 and 0.74, respectively. During the rest of the paper we will use Geotail data for computing the solar wind based parameters.

The beginning of the substorm event, t_b was taken from the southward turning of the IMF B_z component (Figure 1a), the closest one to the substorm onset was selected. The event is thought to end, t_e, when the CL index returned near zero. The duration of the substorm was four hours, from 2:20 UT to 6:20 UT, which is typical (Tanskanen et al., 2002), using the criteria above.

EMPIRICALLY ESTIMATED MAGNETOSPHERIC ENERGY BUDGET

Magnetospheric energy input was computed by using Akasofu's epsilon parameter in SI units (Akasofu, 1981) $\epsilon = 4\pi/\mu_0 \cdot\ vB^2 \sin^4(\theta/2) \cdot\ l_0^2$, where v is the upstream solar wind speed, B the strength of the IMF, θ the IMF clock angle ($\tan\theta = B_y/B_z$) in geocentric solar magnetospheric (GSM) coordinates, and l_0 an empirical parameter to fit the energy input to the total estimated output. Interplanetary magnetic field and solar wind velocity were taken from Geotail observations. In the original works (Perreault and Akasofu, 1978; Akasofu, 1981) the input parameter was scaled to the Joule heating, electron precipitation and ring current with a scaling factor, $l_0 = 7\ R_E$. More recent works (Lu et al., 1998; Knipp et al., 1998; Koskinen and Tanskanen, 2002; Østgaard and Tanskanen, 2002) have shown that the original scaling is somewhat low. Koskinen and Tanskanen (2002) suggest a revision of l_0 from 7 R_E to 9 or 10 R_E, which would increase the estimated energy input by a factor of 1.6 – 2.0. In this work we use the original ϵ with $l_0 = 7\ R_E$ and the rescaled epsilon, ϵ_{scaled}, with $l_0 = 10\ R_E$ (Figure 2a). The revised epsilon covers Joule heating, electron precipitation, ring current and tail processes such as plasmoid release and plasma sheet heating. Total energy needed to feed the substorm is computed by integrating the input power from the beginning to the end of the event. Maximum input energy is $1.0 \cdot 10^{15}$ J from Geotail when the original epsilon is used and twice that when the epsilon is scaled (Figure 2d).

In Figure 2b we show three different proxies for the Ohmic Joule heating. The Ahn et al. (1983) formula converts the westward electrojet index to the power of Joule heating as $P_{JH,Ahn} = 2 \cdot 3 \cdot\ 10^8$ AL. The Richmond et al. (1990) conversion, which includes only winter-time substorms is $P_{JH,Richmond} = 2 \cdot\ 2 \cdot\ 10^8$ AL. All events used by Ahn et al. (1983) took place during summer. The factor of 2 has been added to the Ahn and Richmond formulas to account for two hemispheres. The Østgaard et al. (2002) formula, which

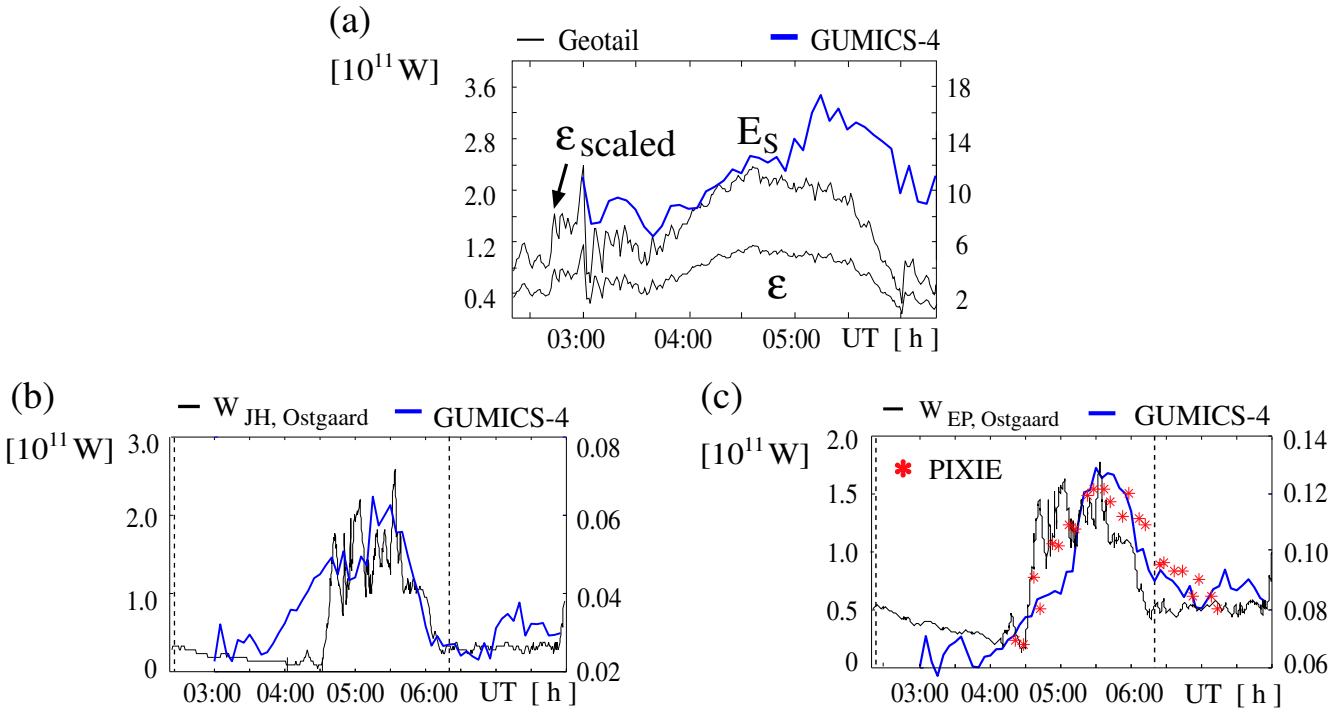

Fig. 3. Comparison of empirical and simulated estimates for energy input (a), Joule heating (b) and electron precipitation (c). Dashed line marks the beginning and the end of the event in b and c. Units for the MHD-simulation results are shown in the right.

takes into account the summer and winter asymmetry, converts the westward electrojet index to power as $P_{JH,Østgaard} = ((0.33\ \mathrm{AE} + (0.21 \cdot\ \mathrm{AE}{+}1.8)) \cdot\ 10^9$. In this study the CL index is used instead of the AL and AE indices. The maximum Joule heating power was about $2.7 \cdot 10^{11}$ W and the total Joule heating energy around 10^{15} J for the Ahn and Østgaard proxies while it was $1.8 \cdot 10^{11}$ W and $0.7 \cdot 10^{15}$ J for the Richmond proxy.

Energy deposition in the northern hemisphere by precipitating electrons has been examined by using observations from the Polar Ionospheric X-ray Imaging Experiment (PIXIE) on board the Polar spacecraft. PIXIE front chamber measurements cover the electron fluxes between 3-30 keV, which is known to give main part of the total northern hemisphere electron precipitation (Østgaard et al., 2002). PIXIE's rear chamber, which was not available during this event, covers the hard tail of the energy spectrum, 30 – 100 keV. However, the hard tail is found to contribute very little to the total energy flux (Østgaard et al., 2002). PIXIE two hemisphere electron flux (Figure 2c) peaks at $1.5{\cdot}10^{11}$ W. Three different empirical proxies, which are shown in Figure 2c are $P_{EP,Ahn} = 2 \cdot 0.8 \cdot\ 10^8$ AL (Ahn et al., 1983), $P_{EP,Spiro} = (1.75 \cdot\ \mathrm{AE}/100nT{+}1.6) \cdot\ 10^{10}$ (Spiro et al., 1982) and $P_{EP,Østgaard} = 2 \cdot (4.4 \cdot\ \sqrt{AL} - 7.6) \cdot\ 10^{19}$ (Østgaard et al., 2002). $P_{EP,Ahn}$ and $P_{EP,Østgaard}$ are multiplied by two for getting the two hemisphere electron precipitation and the CL index is used. These precipitation proxies peak around 0.8, 1.0 and $1.8 \cdot 10^{11}$ W, respectively.

COMPARING EMPIRICAL ESTIMATES AND RESULTS FROM A GLOBAL MHD SIMULATION

A global MHD simulation code, GUMICS-4, (Janhunen, 1996) was used to compute the energy flow through the magnetopause. The steps required to compute the energy flow through the magnetopause in the simulation include the following: First, the magnetopause surface is defined by mapping solar wind flow lines. Once the surface is known, the energy through a surface element is computed by taking the dot product of the simulation total energy and the surface element normal. Finally, the energy through the magnetopause E_s is an integration over the energies through the surface elements. The method is explained in more detail in paper by Palmroth et al. (2003). Figure 3a presents the transferred energy through the

magnetopause in the simulation, E_s, together with the original and rescaled epsilon parameters, which are computed from Geotail observations. The same observations have also been used as input parameters to the GUMICS-4 simulation. As the simulation gives the total energy flowing through the magnetopause, not only energy consumed by the substorm process, it is understandable that $E_s > \epsilon$. However, the simulated and empirically estimated input parameters evolve remarkably similarly in time.

Joule heating in the simulation is computed by using the equation $P_{JH} = \int \mathbf{J} \cdot \mathbf{E}\, dS = \int \Sigma_P\, E^2\, dS$ and electron precipitation in the simulation by using equation in Robinson et al. (1987) described more in detail in the paper by Palmroth et al. (2004). Figure 3b presents the estimates for the Joule heating in simulation and in empirical proxy, when the Østgaard et al. (2002) formula is used. Right vertical axis is for the GUMICS-4 results and the left vertical axis for Østgaard et al. (2002) results. Both estimates for Joule heating peaks between 0515 UT and 0530 UT and after that they both decrease until they cease near the quiet time level about an hour later. The Joule heating in the ionosphere follows closely the changes in the solar wind kinetic energy flux, and most notably the solar wind dynamic pressure (Palmroth et al. 2004). In the simulation the Joule heating increases also as a consequence of increase in the net FAC. PIXIE-based, CL conversion-based and simulation-based electron precipitations are presented in Figure 3c. All three estimates peak very near each other, around 0530 UT. The temporal variation of the PIXIE- and simulation-based precipitation curves match nicely. However, the power levels are quite different.

DISCUSSION AND CONCLUSIONS

Energetics of a 450 nT substorm that occurred on 15 August, 2001 was examined by using empirical power and energy estimates together with power estimates in a global MHD simulation. Examination of input and dissipation proxies show that they give reasonably consistent results. Comparison of the empirical and simulation-based proxies showed that the temporal variation of the curves compare very favorably. Epsilon-based and GUMICS-based energy input estimates show differences mainly in the substorm recovery phase. The epsilon parameter starts to decrease around 0500 UT, while the simulated input, E_S, was still increasing. The differences in the amount of dissipated energy in empirical proxies and in simulation must be investigated further by simulating more events and comparing the results with actual measurements.

The use of empirical proxies introduces minor uncertainty, which can be seen e.g. in Figures 2a, b and c. For some of the variations explanations can be found, such as use of only summer or winter events when the dissipation proxies are formed or using L1 monitors instead of near-magnetopause monitors. Even after these considerations, there is at least a factor 2 between the various estimates, which can not be easily explained. For example the Ahn et al. (1983) electron precipitation power peaks at $0.8 \cdot 10^{11}$ W, while the Østgaard et al. (2002) estimate peaks at $1.8 \cdot 10^{11}$ W. The difference becomes even larger, when real PIXIE data were used. The electron precipitation given by PIXIE peaks around $1.5 \cdot 10^{11}$ W. However, the energy fluxes derived from PIXIE are only in the energy range 3–30 keV, which is then lower that what we would have obtained from the full spectra between 0.1 and 100 keV. When only PIXIE is used the underestimate of about 20 – 30% at substorm onset and expansion phase, but even 50% or more during the growth and recovery phases. Kauristie et al. (1996) showed that replacing the AL by westward electrojet index derived from meridional magnetometer array gives slightly higher values, while the use of westward electrojet indices instead of AE-type of indices cause slight underestimation.

We have employed two quite distinct approaches to estimate both the solar wind energy input and ionospheric energy dissipation. That the input estimates differ is quite understandable as the empirical input function is basically scaled to the inner magnetosphere energy consumption only. It is quite remarkable how similar temporal variation the simulation and empirical proxy-based methods give for the ionospheric dissipation.

ACKNOWLEDGEMENTS

We wish to thank R. Lepping and A. Lazarus for the WIND data, C. Smith and D. McComas for the ACE data, A. Szabo for the IMP 8 data, T. Mukai for the Geotail data, and all institutes maintaining the CANOPUS and the AE magnetometer networks. The work of ET and MP was supported by the Academy of Finland. The study was finished while ET held a National Research Council Postdoctoral research positition at NASA-Goddard Space Flight Center.

REFERENCES

Ahn, B.-H., S.-I. Akasofu, and Y. Kamide The Joule heat production rate and the particle energy injection rate as a function of the geomagnetic indices AE and AL, *J. Geophys. Res., 88*, 6275, 1983.

Akasofu, S.-I., Energy coupling between the solar wind and the magnetosphere, *Space Sci. Rev., 28*, 121–190, 1981.

Hones, E.W., Jr., T. Pytte, and H.I. West Jr., Association of geomagnetic activity with plasma sheet thinning and expansion: A statistical study, *J. Geophys. Res., 89*, 5471, 1984.

Ieda, A. et al., Statistical analysis on the plasmoid evolution with Geotail observations, *J. Geophys. Res., 103*, 4453, 1998.

Janhunen, P., GUMICS-3 - A global ionospheric-magnetospheric coupling simulation with high ionospheric resolution, in, *Proc. Environmental Modelling for Space-Based Applications, Sept. 18-20, 1996*)ESTEC, The Netherlands, ESA SP-392, 1996.

Koskinen H.E.J. and E. Tanskanen, Magnetospheric energy budget and the epsilon parameter, J. Geophys. Res., 107(A11), 1415, doi:10029/2002JA009283, 2002

Kauristie, K. et al., What can we tell about auroral electrojet activity from a single meridional magnetometer chain, *Ann. Geophys., 14*, 1177-1185, 1996.

Knipp D.J. et al., An overview of the early November 1993 geomagnetic storm, *J. Geophys. Res., 103*, 26197, 1998.

Lu, G. et al., Global energy deposition during the January 1997 magnetic cloud event, *J. Geophys. Res., 103*, 11685, 1998.

Østgaard, N. and E. I. Tanskanen, Energetics of isolated and stormtime substorms, *AGU Geophysical Monographs, Disturbances in Geospace: The storm-substorm relationship, 142*, 2004.

Østgaard, et al., A relation between the energy deposition by electron precipitation and geomagnetic indices during substorms, *J. Geophys. Res.,107*, 10.1029/ 2001JA002003, 2002.

Palmroth, M., et al., Stormtime energy transfer in global MHD simulation, *J. Geophys. Res., 108, A1*, SMP 24-1, CiteID 1048, DOI 10.1029/2002JA009446, 2003.

Palmroth, M., P. Janhunen, and T.I. Pulkkinen, Ionospheric energy input as a function of solar wind parameters as determined: global MHD simulation results, *Ann. Geophysicae, 22, 549*, 2004.

Perreault, P., and S.-I. Akasofu, A study of geomagnetic storms, *Geophys. J. R. Astr. Soc., 54*, 547, 1978.

Spiro R.W., P.H. Reiff, and L.J. Maher, Jr., Precipitating electron energy flux and auroral zone conductances - an empirical model, *J. Geophys. Res., 87*, 8215, 1982.

Richardson, I.G et al., Plasmoid-associated energetic ion bursts in the deep geomagnetic tail - Properties of plasmoids and the postplasmoid plasma sheet, *J. Geophys. Res.,92*, 9997, 1987.

Slavin J.A. et al., Substorm accociated traveling compression regions in the distant tail - ISEE-3 geotail observations, *Geophys. Rev. Lett., 11*, 657, 1984.

Slavin, J.A. et al., ISEE 3 observations of traveling compression regions in the earth's magnetotail, *J. Geophys. Res., 98*, 15425, 1993.

Tanskanen, E. et al., Substorm energy budget during low and high solar activity: 1997 and 1999 compared, *J. Geophys. Res., 107*, 101029/2001JA900153, 2002.